Available online at www.sciencedirect.com
SCIENCE DIRECT®
Biochemical Pharmacology 65 (2003) 783–793
Biochemical Pharmacology
www.elsevier.com/locate/biochempharm

ET_A receptor-mediated Ca^{2+} mobilisation in H9c2 cardiac cells

Francesca Ceccarelli[a], Maria C. Scavuzzo[b], Laura Giusti[a], Gianni Bigini[a], Barbara Costa[a], Vittoria Carnicelli[c], Riccardo Zucchi[c], Antonio Lucacchini[a], Maria R. Mazzoni[a,*]

[a]*Dipartimento di Psichiatria, Neurobiologia, Farmacologia e Biotecnologie, Università di Pisa, Pisa, Italy*
[b]*Dipartimento di Morfologia Umana e Biologia Applicata, Università di Pisa, Pisa, Italy*
[c]*Dipartimento di Scienze dell'Uomo e dell'Ambiente, Università di Pisa, Pisa, Italy*

Received 25 July 2002; accepted 19 November 2002

Abstract

Expression and pharmacological properties of endothelin receptors (ETRs) were investigated in H9c2 cardiomyoblasts. The mechanism of receptor-mediated modulation of intracellular Ca^{2+} concentration ($[Ca^{2+}]_i$) was examined by measuring fluorescence increase of Fluo-3-loaded cells with flow cytometry. Binding assays showed that [^{125}I]endothelin-1 (ET-1) bound to a single class of high affinity binding sites in cardiomyoblast membranes. Endothelin-3 (ET-3) displaced bound [^{125}I]ET-1 in a biphasic manner, in contrast to an ET_B-selective agonist, IRL-1620, that was ineffective. The ET_B-selective antagonist, BQ-788, inhibited [^{125}I]ET-1 binding in a monophasic manner and with low potency. An ET_A-selective antagonist, BQ-123, competed [^{125}I]ET-1 binding in a monophasic manner. This antagonist was found to be 13-fold more potent than BQ-788. Immunoblotting analysis using anti-ET_A and -ET_B antibodies confirmed a predominant expression of the ET_A receptor. ET-1 induced a concentration-dependent increase of Fluo-3 fluorescence in cardiomyoblasts resuspended in buffer containing 1 mM $CaCl_2$. Treatment of cells with antagonists, PD-145065 and BQ-123, or a phospholipase C-β inhibitor, U-73122, abolished ET-1-mediated increases in fluorescence. The close structural analogue of U-73122, U-73343, caused a minimal effect on the concentration–response curve of ET-1. ET-3 produced no major increase of Fluo-3 fluorescence. Removal of extracellular Ca^{2+} resulted in a shift to the right of the ET-1 concentration–response curve. Both the L-type voltage-operated Ca^{2+} channel blocker, nifedipine, and the ryanodine receptor inhibitor, dantrolene, reduced the efficacy of ET-1. Two protein kinase C inhibitors reduced both potency and efficacy of ET-1. Our results demonstrate that ET_A receptors are expressed and functionally coupled to rise of $[Ca^{2+}]_i$ in H9c2 cardiomyoblasts. ET-1-induced $[Ca^{2+}]_i$ increase is triggered by Ca^{2+} release from intracellular inositol 1,4,5-trisphosphate-gated stores; plasma membrane Ca^{2+} channels and ryanodine receptors participate in sustaining the Ca^{2+} response. Regulation of channel opening by protein kinase C is also involved in the process of $[Ca^{2+}]_i$ increase.

Keywords: H9c2 cells; Endothelin receptors; IP_3 receptors; Ryanodine receptors; Ca^{2+} channels

* Corresponding author. Tel.: +39-50-24092; fax: +39-50-503534.
E-mail addresses: maria.mazzoni@vanderbilt.edu, mariarm@farm.unipi.it (M.R. Mazzoni).

Abbreviations: ET, endothelin; ET-1, endothelin-1; ETRs, endothelin receptors; PLC, phospholipase C-β; IP_3, inositol 1,4,5-trisphosphate; DG, diacylglycerol; IP_3R, IP_3 receptor; RyR, ryanodine receptor; $[Ca^{2+}]_i$, intracellular Ca^{2+} concentration; $[Ca^{2+}]_c$, cytoplasmic free Ca^{2+} concentration; VOCC, voltage-operated Ca^{2+} channel; PKC, protein kinase C; PMSF, phenylmethanesulphonyl fluoride; BQ-123, cyclo(D-α-Asp-Pro-D-Val-Leu-D-Trp); BQ-788, *N*-[*N*-[*N*-[(2,6-dimethyl-1-piperidinyl)carbonyl]-4-methyl-Leu]-1-(methoxycarbonyl)-D-Trp]-D-norLeu; IRL-1620, *N*-Suc-[Glu^9,Ala^{11,15}]-endothelin-1 (8–21); Fluo-3 AM, Fluo-3 acetoxymethyl ester; PD-145065, *N*-acetyl-α-[10,11-dihydro-5*H*-dibenzo[*a*,*d*]cycloepta-dien-5-yl]-D-Gly-Leu-Asp-Ile-Ile-Trp; U-73122, 1-[6-[[17β-3-methoxyestra-1,3,5(10)-trien-17-yl]amino]hexyl]-1*H*-pyrrole-2,5-dione; U-73343, 1-[6-[[17β-3-methoxyestra-1,3,5(10)-trien-17-yl]amino]hexyl]-2,5-pyrrolidine-dione; PE, phycoerythrin; GADPH, glyceraldehyde-3-phosphate dehydrogenase; OD, optical density.

1. Introduction

ET-1, a 21-residue peptide, is recognised as a potent vasoconstrictor [1]. In humans three distinct genes encode for three endothelin (ET) isopeptides, ET-1, ET-2 and ET-3 [2]. Of these isopeptides, ET-1 is the only form constitutively released by ET cells, but many other cells are now known to have the ability to produce ETs (for reviews see [3–5]). Besides modulating the smooth muscle tone, ETs also stimulate cell proliferation in all tissues. All biological effects are elicited by binding and activation of specific cell surface receptors (endothelin receptors (ETRs)), which belong to the large family of G protein-coupled receptors. Pharmacological studies and molecular cloning [5] have revealed the existence of at least two ETR subtypes with

0006-2952/02/$ – see front matter
doi:10.1016/S0006-2952(02)01624-6

different cell distribution and roles in regulating the vascular tone, termed ET_A and ET_B receptors [3]. ETR activation leads to second messenger generation through a variety of signal transduction pathways, including activation of phospholipase C-β (PLC) [5], A_2 and D [5–7], inhibition or activation of adenylyl cyclase [5], activation of both Ca^{2+}-permeable non-selective cation channels [5,8] and L-type voltage-operated Ca^{2+} channels (VOCCs) [3,5] and regulation of Na^+/H^+ exchange activity [5].

ETs have direct effects on cardiac tissue [6] that synthesises, stores and releases ET-1 [9]. Both binding studies [9] and *in situ* hybridisation studies [8] have shown a wide expression of ET_A and ET_B receptors in human atrial and ventricular myocardium. However, homogenous populations of right atrial [10] or left [11] ventricular cardiomyocytes demonstrated a high proportion of ET_A receptor binding sites (86–90%) than that found in tissue preparations. In adult and neonatal rat ventricular cardiomyocytes a homogenous population of ET_A receptors coupled to multiple effector pathways (i.e. activation of PLC and inhibition of adenylyl cyclase) has been described [12,13].

The clonal cardiac cell line H9c2 derived from embryonic rat heart has been used as an experimental model to study L-type VOCCs with cardiac-specific characteristics [14] and the ontogenic expression of these channels [15]. When cultured in the presence of a low foetal bovine serum (FBS) concentration, H9c2 cardiomyoblasts differentiate to myotubes expressing both cardiac and skeletal L-type VOCCs [15] and ryanodine receptor (RyR) Ca^{2+} release channels [16]. These cardiomyoblasts also express V_1 receptors resulting in vasopressin-induced mobilisation of Ca^{2+} from intracellular stores, activation of PLC, PLA_2 and the p42 MAP kinase [17–19]. In addition, vasopressin stimulates H9c2 cell hypertrophy [20]. Thus, this cardiac cell line is a particularly valuable tool for the investigation of receptor-mediated modulation of $[Ca^{2+}]_i$ during cell growth and differentiation.

The present study was undertaken in H9c2 cadiomyoblasts in order to dissect the signal transduction pathways activated by ET-1, a major hypertrophic agent for cardiomyocytes. Here, we present evidence that the ET_A receptor subtype is preferentially expressed in this cell line and functionally coupled to an increase of $[Ca^{2+}]_i$. Receptor-mediated $[Ca^{2+}]_i$ variations are known to be triggered and sustained by Ca^{2+} release from intracellular inositol 1,4,5-trisphosphate (IP_3)-sensitive stores, but the participation of plasma membrane Ca^{2+} channels and RyRs is also obvious in this event. In addition, protein kinase C (PKC) is involved in modulating Ca^{2+} channel opening. These findings demonstrate the presence of a functional intact signal transduction machinery which couples ET_A receptors to elevation of $[Ca^{2+}]_i$ in rat cardiomyoblasts and highlight integrated responses of intracellular and plasma membrane Ca^{2+} channels. The H9c2 cell line may represent a useful model to study ETR expression and coupling to signal transduction pathways during differentiation and hypertrophic responses. The importance of this cellular model also arises from the consideration that the cardiac ET-1/ET_A receptor system is upregulated in left ventricular hypertrophy [21,22].

2. Materials and methods

2.1. Cell culture

H9c2 (2-1) rat cardiomyoblasts were propagated in Dulbecco's modified Eagle's medium (DMEM) supplemented with 10% FBS, 1 mM pyruvate, 100 units/mL penicillin, 100 μg/mL streptomycin and 0.02 mg/mL 2,4-difluoro-α,α^1-bis(1*H*-1,2,4-triazol-1-ylmethyl)benzyl alcohol (fluconazole), at 37° in a humidified atmosphere containing 5% CO_2 and subcultured before confluence.

2.2. Membrane preparation

Subconfluent monolayers (passages 16–24) were washed with 8.1 mM Na_2HPO_4, 1.5 mM KH_2PO_4, pH 7.4, 136.8 mM NaCl and 2.7 mM KCl (PBS), harvested with a cell scraper and collected by centrifugation at 1000 *g*. Cells were homogenised in 10 mM Tris–HCl, pH 7.3, containing 1 mM EDTA, 160 μg/mL benzamidine, 200 μg/mL bacitracin, 0.1 mM phenylmethanesulphonyl fluoride (PMSF) and 20 μg/mL trypsin inhibitor (buffer A) using a Polytron homogeniser. The homogenate was centrifuged at 48,000 *g* at 4° for 30 min. The resulting pellet was resuspended in buffer A, homogenised and centrifuged as described earlier. The membrane pellet was stored in aliquots at −80° until the time of assay. Protein concentration was determined by the method of Lowry *et al*. [23], using BSA as standard.

2.3. Binding assays

[^{125}I]ET-1 binding assays were performed as described by Mazzoni *et al*. [24], with some modifications. Briefly, cell membranes (~7.5 μg of proteins) were incubated with [^{125}I]ET-1 (~20 pM) in 250 μL of 20 mM Tris–HCl buffer, pH 7.4, at 37°, containing 2 mM EDTA, 0.1 mM bacitracin, 0.1 mM PMSF, 1 μg/mL leupeptin, 5 μg/mL aprotinin (buffer B) and 0.08 mg/mL BSA for 2 hr at 37°. After incubation, the reaction was stopped with 3 mL of ice-cold 50 mM Tris–HCl, pH 7.3, at 4°, containing 0.1 mM bacitracin (buffer C). Membrane bound radioactivity was separated from the free ligand by filtration through Whatman GF/C filters that had been pre-soaked in buffer C containing 2 mg/mL BSA. The filters were washed three times with 3 mL of buffer C. Non-specific binding was defined as the binding that occurred in the presence of an excess of ET-1 (100 nM). At 20 pM [^{125}I]ET-1, specific binding was 95% of total binding. Dilution and competition binding experiments were performed by incubating membranes with [^{125}I]ET-1 in the presence

and absence of various concentrations of the unlabelled ligands: ET-1 (0.002–5 nM), ET-3 (0.005–1000 nM), cyclo-(D-α-Asp-Pro-D-Val-Leu-D-Trp (BQ-123) (2.5–1000 nM), *N*-[*N*-[*N*-[(2,6-dimethyl-1-piperidinyl)carbonyl]-4-methyl-Leu]-1-(methoxycarbonyl)-D-Trp]-D-norLeu (BQ-788) (1–1000 nM) and *N*-Suc-[Glu^{9},$Ala^{11,15}$]ET-1 (8–21) (IRL-1620) (0.01–100 nM). Stock solutions of ET-1 and ET-3 were prepared in buffer B; other compounds were dissolved in DMSO and then diluted in buffer B to the desired concentration. In binding assays, the final concentration of DMSO never exceeded 0.2%. Within this concentration, DMSO did not influence [^{125}I]ET-1 binding to membranes.

[^{3}H]Ryanodine binding assays were performed as described by Zucchi *et al*. [25]. In each assay, the concentration of [^{3}H]ryanodine (10 Ci/mmol) was 40 nM.

2.4. Western blotting

SDS–polyacrylamide gel (4–20%) electrophoresis of cardiomyoblast membrane proteins (∼30 μg of protein in each well) was carried out according to the method of Laemmli [26]. Proteins were electroblotted from SDS–polyacrylamide gels to nitrocellulose (0.2 μm), then incubated overnight at 4° in PBS (10 mM NaH_2PO_4, pH 7.4, 0.9% NaCl) containing 3% low fat dried milk and 0.2% Tween 20 (PBS/milk). The nitrocellulose membrane was then incubated in PBS/milk containing sheep polyclonal anti-ET_A or -ET_B antibodies (10–20 μg/mL) for 1 hr at room temperature followed by four washes with PBS/milk. Afterwards, nitrocellulose was incubated in PBS/milk containing peroxidase-labelled secondary antibody (1:8000 dilution) for 1 hr at room temperature. The washing step was repeated as described earlier, followed by two washes with PBS and one with distilled water. The immunoblot was incubated in an enhanced chemiluminescent substrate for 1 min at room temperature and then briefly exposed to a Kodak Biomax ML film. The intensity of immunoreactive bands was quantified by densitometric scanning with a Bio-Rad Model GS-670 Imaging Densitometer (Bio-Rad Laboratories).

2.5. $[Ca^{2+}]_i$ measurements

Subconfluent cell cultures in 60-mm plastic petri dishes were incubated for 30 min at 37° in the absence of light in loading buffer (20 mM HEPES, pH 7.4, 130 mM NaCl, 5 mM KCl, 2 mM $CaCl_2$, 1 mM $MgSO_4$, 0.8 mM Na_2HPO_4, 0.2 mM NaH_2PO_4, 25 mM mannose and 1 mg/mL BSA) containing 2 μM Fluo-3 acetoxymethyl ester (Fluo-3 AM) and 0.008% Pluronic F-127 dissolved in DMSO. After incubation, the monolayers were washed in detaching buffer (10 mM HEPES, pH 7.4, 140 mM NaCl, 5 mM KCl, 0.55 mM $MgCl_2$ and 3 mM EDTA) and incubated in the same buffer at 37° for 10 min. Detached cells were harvested by low-speed centrifugation (1000 *g*), resuspended in assay buffer (10 mM HEPES, pH 7.4, 140 mM NaCl, 5 mM KCl, 0.55 mM $MgCl_2$ and 1 mM $CaCl_2$) and analysed on a FACScan flow cytometer with the CellQuest software (Becton Dickinson Labware). Polystyrene spheres were used for calibration and normalisation of the flow cytometer prior of each experiment. In each sample 5000 events were recorded and analysed using FACSComp software. A blue excitation at 488 nm from an argon-ion laser was used for three-colour analysis of Fluo-3 green, YO-PRO-1 iodide green and propidium iodide red fluorescences. The forward- and right-angle light scatters (FSC and SSC) were used to gate the cells. Fluo-3 was excited at 488 nM with Fluo-3 emission detected at 525 nm. YO-PRO-1 was excited at 491 nm and green emission was detected at 509 nm while propidium iodide was excited at 535 nm and red emission detected at 617 nm. FSC, SSC and Fluo-3 fluorescences were displayed on a linear scale whereas those of propidium iodide YO-PRO-1 were represented on a logarithmic scale. The "time" parameter was activated on a scale of 1000 ms (100 s/channel). Cells were analysed at typical rates of 100–150 cells/s. Data were collected in histograms displaying the ratio of Fluo-3 fluorescence vs. time and YO-PRO-1 fluorescence vs. propidium iodine fluorescence.

To convert Fluo-3 fluorescence data into absolute $[Ca^{2+}]_i$, a calibration procedure was carried out on each experiment as described by Vandenberghe and Ceuppens [27]. To obtain the maximal fluorescence, cells were selectively permeabilised to divalent cations using 10 μM ionomycin in assay buffer without $MgCl_2$. The minimal fluorescence was determined after the addition of 2 mM $MnCl_2$.

To determine the cellular response, baseline, unstimulated measurements were followed by addition of various concentration of ET-1 (0.25–5000 nM) or ET-3 (1–5000 nM). The cell flow was halted during this addition and sample measurement was carried out within 2–3 s. In the experiments performed in the absence of extracellular Ca^{2+}, 1 mM $CaCl_2$ was replaced with 1 mM EGTA in the assay buffer. To test the effects of ETR antagonists and a L-type VOCC blocker, the unstimulated baseline measurements were followed by addition of 1 μM *N*-acetyl-α-[10,11-dihydro-5*H*-dibenzo[*a*,*d*]cycloeptadien-5-yl]-D-Gly-Leu-Asp-Ile-Ile-Trp (PD-145065), BQ-123 or nifedipine, after which various concentrations of ET-1 (1–5000 nM) were added. Dantrolene (100 μM), an inhibitor of RyRs, was added together with Fluo-3 AM to cell cultures and then incubated as described earlier. Following cell detachment, basal and ET-1-stimulated fluorescence measurements were performed as indicated. In experiments designed to understand the role of PLC, adenylyl cyclase or PKC activation, cell suspensions were preincubated for 5 min at room temperature in the presence of 10 μM 1-[6-[[17β-3-methoxyestra-1,3,5(10)-trien-17-yl]amino]hexyl]-1*H*-pyrrole-2,5-dione (U-73122) (inhibitor of PLC), 1-[6-[[17β-3-methoxyestra-1,3,5(10)-trien-17-yl]amino]hexyl]-2,5-pyrrolidine-dione (U-73343) (structural analogue of U-73122, but inactive as inhibitor

of PLC), 1 μM forskolin (activator of adenylyl cyclase) or 2 μM chelerythrine (PKC inhibitor) before stimulation with various concentrations of ET-1 (1–5000 nM). To further test a possible role of PKC in ET-1-induced variations of $[Ca^{2+}]_i$ in cardiomyoblasts, two other PKC inhibitors were used, calphostin C and a PKC pseudosubstrate peptide, myr-Phe-Ala-Arg-Lys-Gly-Ala-Leu-Arg-Gln (20–28 sequence from PKC-α and PKC-β) (myr-PKC(20–28)). Subconfluent cell cultures were incubated in loading buffer containing 50 nM calphostin C for 30 min at room temperature under fluorescent light. Subsequently, cells were incubated for 30 min at 37° followed by addition of 2 μM Fluo-3 AM and further incubation at 37° for 30 min. Alternatively, cardiomyoblasts were incubated in the presence of myr-PKC(20–28) (10 μM) and Fluo-3 for 30 min at 37°. At the end of this incubation period, cells were detached and both basal and ET-1-stimulated fluorescence measurements were performed as described earlier.

Stock solutions of BQ-123, forskolin, dantrolene, U-73122, U-73343 and calphostin C were prepared in DMSO. In cell assays, the final concentration of DMSO never exceeded 0.1%.

In order to estimate the proportion of apoptotic and necrotic cells in our samples, detached cardiomyoblasts resuspended in assay buffer (see earlier description) containing YO-PRO-1 dye and propidium iodide were analysed by the flow cytometer as described earlier. Three cell populations were distinguished on the basis of their fluorescence as follows: apoptotic cells showed green fluorescence, dead cells showed red and green fluorescence while live cells showed little or no fluorescence. To detect early apoptotic cells by flow cytometry, the binding method of the fluorochrome phycoerythrin (PE)-labelled annexin V to membrane phosphatidylserine was used [28]. Briefly, cardiomyoblasts were treated with calphostin C or DMSO and then detached as described earlier. Cells were centrifuged and resuspended in 10 mM HEPES, pH 7.4, 150 mM NaCl, 5 mM KCl, 1 mM $MgCl_2$ and 1.8 mM $CaCl_2$. After addition of recombinant annexin V-PE, cells were incubated at room temperature for 15 min and centrifuged. Following a washing step with PBS containing 0.01% NaN_3, cells were resuspended in this buffer and analysed by the flow and analysed on a FACScan flow cytometer.

2.6. Reverse transcriptase–polymerase chain reaction (RT–PCR) amplification and sequencing

Total RNA was prepared from subconfluent H9c2 cell cultures using the RNeasy Mini Kit. Leading strand cDNA was synthesised from 1 μg of DNase-treated RNAs in 50 μL and cDNA were amplified using HSEnhanced Avian Reverse Transcriptase Kit. Incubation at 42° for 50 min was followed by denaturation for 2 min at 94°. PCR reactions were carried out for 35 cycles for 15 s at 94° and anneal-extending for 1 min at 68° followed by a final extension for 5 min at 68°. Two pairs of PCR primers (5 μM) were used. One primer couple was specific for the *RyR*$_2$ gene (forward primer, 5′-AAGGAGAGCATTTCC-CGTACGAGC-3′; reverse primer, 5′-AAAGAGGCCTG-CTTGCGACAGA-3′) while the control primer pair was designed to amplify rat glyceraldehyde-3-phosphate dehydrogenase (GADPH) (forward primer, 5′-GCAACTCC-CATTCTTCCACCTTTGA-3′; reverse primer, 5′-TTGG-AGGCCATGTAGGCCATGA-3′). Each pair contained a fluorescent dye-labelled primer (6-FAM-tagged). Thus, the RT–PCR allowed the simultaneous amplification of a 119-bp fragment related to RyR_2 and a 135-bp fragment related to GADPH. The fragments were revealed using the ABI PRISM 310 Genetic Analyzer (Applied Biosystems) and analysed with the GeneScan program (Applied Biosystems).

2.7. Analysis of data

The Cell Quest computer program (Becton Dickinson) was used to collect and perform statistical analysis of fluorescence experiments. Fluorescence data were analysed by non-linear least squares fitting, using the sigmoidal dose–response equation of the GraphPad Prism Version 3.00 computer program (GraphPad Software). The EC_{50} values were derived from the resulting concentration–response curves. A non-linear multipurpose curve-fitting computer program (EBDA/LIGAND; Elsevier-Biosoft) [29] was used to transform dilution experiments of [^{125}I]ET-1 with unlabelled ET-1. Displacement, dilution and saturation data were analysed and fitted using either competition or hyperbolic binding equations of the GraphPad Prism Version 3.00 computer program. Single- and multiple-site models were statistically compared to determine the best fit and differences between models were tested by comparing the residual variance using a partial F test and a significance level of $P < 0.05$ (GraphPad Prism Version 3.00). The IC_{50} values obtained from displacement and dilution curves were converted to K_i values by the Cheng and Prusoff equation [30]. Values represent the mean ± SEM of at least three experiments. Mean and SEM values were calculated using the statistical analysis of GraphPad Prism Version 3.00 computer program.

2.8. Materials

H9c2 (2-1) rat cardiomyoblasts at passage 12 were obtained from the American Type Culture Collection (ATCC). [^{125}I]ET-1 (2200 Ci/mmol) and [^{3}H]ryanodine (60 Ci/mmol) were purchased from NEN Life Science Products. ET-1, ET-3, BQ-788, PD-145065, IRL-1620, sheep polyclonal anti-ET_A and -ET_B antibodies were from Alexis Corp. BQ-123, forskolin, ionomycin, aprotinin, leupeptin, benzamidine, DMEM, calphostin C, chelerythrine, nifedipine, dantrolene, propidium iodine, nitrocellulose membranes, DNase and the HSEnhanced Avian Reverse Transcriptase Kit were products of Sigma Chemical Co. Bacitracin and PMSF were purchased from

Fluka Chemie AG. SDS–polyacrylamide (4–20%) minigels were from Bio-Rad Laboratories, while the ECL western blotting detection reagent was from Amersham Pharmacia Biotech. The anti-sheep IgG antibody was purchased from Calbiochem-Novabiochem Corp. Recombinant annexin V-PE was from MedSystems Diagnostics GmbH. The RNeasy Mini Kit was purchased from Qiagen Inch. Fluo-3 AM, Pluronic F-127 and YO-PRO-1 iodine were obtained from Molecular Probes, Inc. FBS, penicillin and streptomycin were products of Gibco. Fluconazole (Diflucan®) was obtained from Roering-Pfizer. U-73122, U-73342 and myr-PKC(20–28) were purchased from Biomol Research Laboratories, Inc. Other agents and reagents were from standard commercial sources.

3. Results

3.1. Characterization of [^{125}I]ET-1 binding sites in H9c2 cardiomyoblasts

[^{125}I]ET-1 bound to membranes prepared from H9c2 rat cardiomyoblasts in a specific manner. All assays were performed at membrane protein concentrations (30–50 μg/mL) that were within the linear range of their concentration curve. Time course experiments showed that [^{125}I]ET-1 binding reached equilibrium by 2 hr at 37° at the ligand (20 pM) and protein (30 μg/mL) concentrations used (data not shown).

Dilution experiments of [^{125}I]ET-1 with unlabelled ET-1 and transformation of data demonstrated that specific

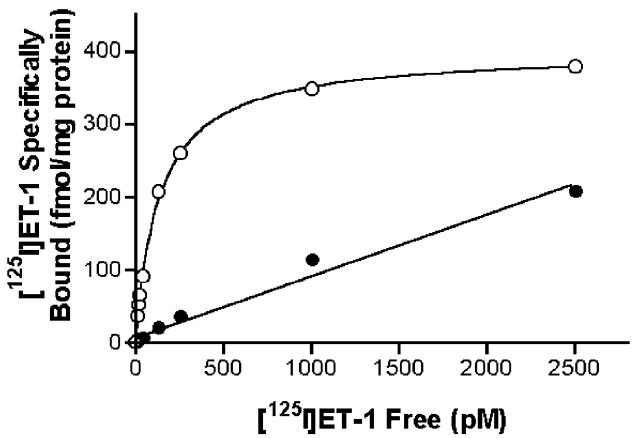

Fig. 1. Equilibrium binding of [^{125}I]ET-1 to H9c2 cardiomyoblast membranes. The saturation isotherm was obtained by transformation of dilution binding data; (○) specific binding, (●) non-specific binding. Membranes (7.5 μg of protein) were incubated with [^{125}I]ET-1 (20 pM) in the presence and absence of increasing concentrations of unlabelled ET-1 ranging from 0.002 to 5 nM as described under "Section 2". Non-specific binding was measured in the presence of 100 nM ET-1. Values shown are means from a representative experiment performed in duplicate and repeated two additional times with similar results. For this experiment, the K_D and B_{max} values were 136.21 pM and 398 fmol/mg protein, respectively. The curve and line were fitted using the non-linear and linear regression analysis of computer program GraphPad Prism Version 3.00.

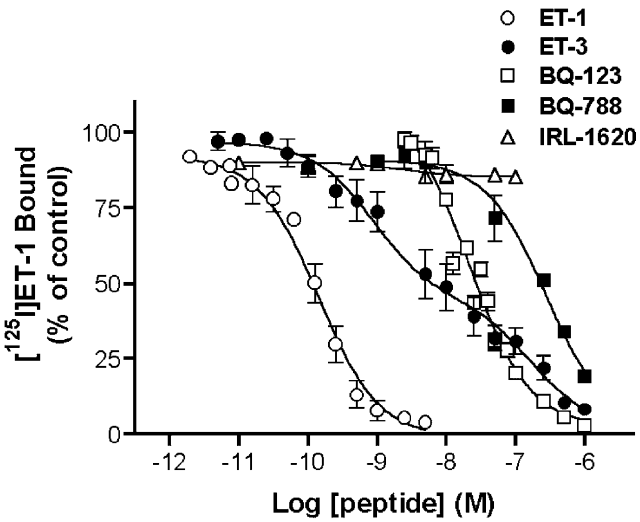

Fig. 2. Competition of [^{125}I]ET-1 binding to H9c2 cardiomyoblast membranes by unlabelled ET-1, ET-3, BQ-123, BQ-788 and IRL-1620. Membranes (7.5 μg of protein) were incubated in duplicate with [^{125}I]ET-1 (20 pM) in the presence and absence of increasing concentrations of ligands, as described under "Section 2". Non-specific binding was measured in the presence of 100 nM ET-1. The non-linear regression analysis of the GraphPad Prism computer program was used to fit the concentration–response curves and derive IC_{50} values. The data points represent the means ± SEM of at least three independent experiments.

binding was saturable (Fig. 1). Analysis of saturation data using the non-linear curve-fitting technique of GraphPad Prism Version 3.0 program revealed that the best fit observed was for one-site model. The derived K_D and B_{max} values were 123.30 ± 12.90 pM and 382 ± 16 fmol/mg protein (N = 3), respectively. As expected, ET-1 dilution data were represented by a monophasic competition curve fitted by one-site model (Fig. 2). In Table 1, the derived inhibition constant (K_i) is shown. The competition curve of [^{125}I]ET-1 binding by ET-3 was biphasic with a significant better fit for a two-site than one-site model (Fig. 2) suggesting the presence of two binding sites. This curve was shifted to the right respect to ET-1 dilution curve. In addition, specific binding was not completely inhibited even at 1 μM ET-3. To perform a pharmacological characterisation of ETRs in rat cardiomyoblast membranes the inhibition of [^{125}I]ET-1 binding by an ET_A-selective antagonist (BQ-123), an ET_B-selective antagonist (BQ-788) or agonist (IRL-1620) was investigated. The antagonists inhibited specific binding in a concentration-dependent manner (Fig. 2) while the agonist, IRL-1620, was not effective within the concentration range (0.01–100 nM) tested (Fig. 2). The competition curve of BQ-123 was monophasic represented by one-site model but shifted to the right respect to ET-1 dilution curve. A complete inhibition of [^{125}I]ET-1 binding was reached at 1 μM BQ-123. The ET_B-selective antagonist, BQ-788, was a less potent inhibitor than BQ-123 (Fig. 2). The competition curve was monophasic fitted by one-site model but this antagonist did not block approximately 20% of [^{125}I]ET-1 binding sites at the maximal concentration (1 μM) tested. Table 1 summarises the percentage distribution of binding

Table 1
Inhibition of [^{125}I]ET-1 binding to H9c2 cardiomyoblast membranes by agonist and antagonist ligands

Ligand	K_H (nM)	R_H (%)	K_L (nM)	R_L (%)	R_N (%)
ET-1	0.12 ± 0.02	100.00	–	–	–
ET-3	0.75 ± 0.08	54.45	147.39 ± 15.47	45.55	–
BQ-123	18.23 ± 2.17	100.00	–	–	–
BQ-788	236.98 ± 24.82	80.80	–	–	19.20
IRL-1620	–	–	–	–	100.00

Cardiomyoblast membranes (~7.5 μg) were incubated with [^{125}I]ET-1 (~20 pM) in the presence and absence of increasing concentrations of ligands, as described in "Section 2". The non-linear regression analysis of the GraphPad Prism computer program was used to fit the dose–response curves and derive the IC_{50} values. The IC_{50} values were converted to K_i values by the Cheng and Prusoff equation [30]. K_H and K_L are the K_i values for the high and low affinity sites while R_H and R_L indicate their respective percentage of distribution. R_N represents the estimated percentage of binding sites that are not blocked by the competing ligand. All K_i values are expressed as means ± SEM of at least three experiments, each performed in duplicate.

sites and K_i values for all compounds tested as competitors of [^{125}I]ET-1 binding to cardiomyoblast membranes.

3.2. Immunoblotting resolution of ET_A and ET_B receptors

To verify the expression of ETR subtypes in H9c2 cells, we performed immunoblotting analysis of cardiomyoblast membrane proteins using either an anti-ET_A or -ET_B affinity purified antiserum. The antibodies were raised against 13-amino acid peptides from the carboxyl-terminal sequence of ET_A and ET_B receptors. The two sequences share just one amino acid in common. In separate lanes, the antisera recognised protein bands of similar molecular mass, indicating that both receptor subtypes were expressed in cardiomyoblasts (Fig. 3, panel a). The ET_A receptor immunoreactive band was particularly intense and corresponded to a 39–40 kDa (N = 3) protein while the ET_B band, which similarly migrated as a 39–41 kDa (N = 3) protein, was barely detectable. Densitometric scanning showed that the OD of the ET_A band was approximately 7-fold higher than that of the ET_B band (Fig. 3, panel b). In addition, less intense bands were visible with both anti-ET_A and -ET_B antibodies. In the ET_A lane, these bands migrated as ~61 and 95 kDa proteins while in the ET_B lane they showed relative molecular masses of ~32 and 59–74 kDa, respectively. While the ~32 kDa band may represent a product of proteolytic degradation of the mature ET_B receptor polypeptide [5], the higher molecular mass bands may result from a different profile of receptor glycosylation [5] and immature receptor forms still containing the signal peptide as part of their amino-terminal tail [31]. Indeed, affinity-labelling studies of ETRs showed the heterogeneity of their molecular mass [5].

3.3. ET-stimulated Ca^{2+} signalling in H9c2 cardiomyoblasts

ET-1 acting through ET_A receptors stimulates PLC activation leading to IP_3 and diacylglycerol (DG) production. The integrity of the signal transduction pathway activated by ET_A receptors in cadiomyoblasts was examined evaluating intracellular Ca^{2+} mobilisation. Among cardiomyoblast population, Fluo-3 fluorescence was recorded from those cells within the viable cell gate. Average values of viable, necrotic and apoptotic cells were 53.68 ± 3.12, 35.99 ± 2.55 and 8.94 ± 1.95% (N = 15), respectively. In addition, a calibration procedure was used in each experiment to

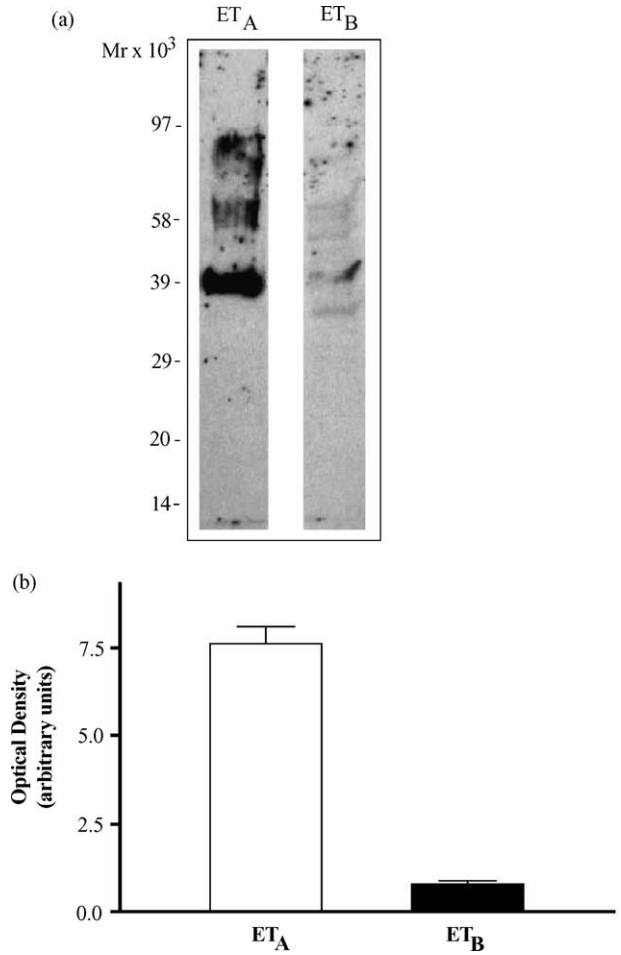

Fig. 3. Immunoblot analysis of ET_A and ET_B receptors in H9c2 cardiomyoblast membranes. Membrane proteins (30 μg) were separated by SDS–polyacrylamide (4–20%) gel electrophoresis and transferred onto nitrocellulose. Antibody binding to ETRs was detected as described under "Section 2". (a) A representative immunoblot. Molecular mass standards are indicated on the left side. (b) The density of the immunoreactive bands was measured using the Bio-Rad Model GS-670 Imaging Densitometer. The OD, expressed as arbitrary units, represents the integrated area of ~39–41 kDa bands. Each value is the means ± SEM of three independent experiments.

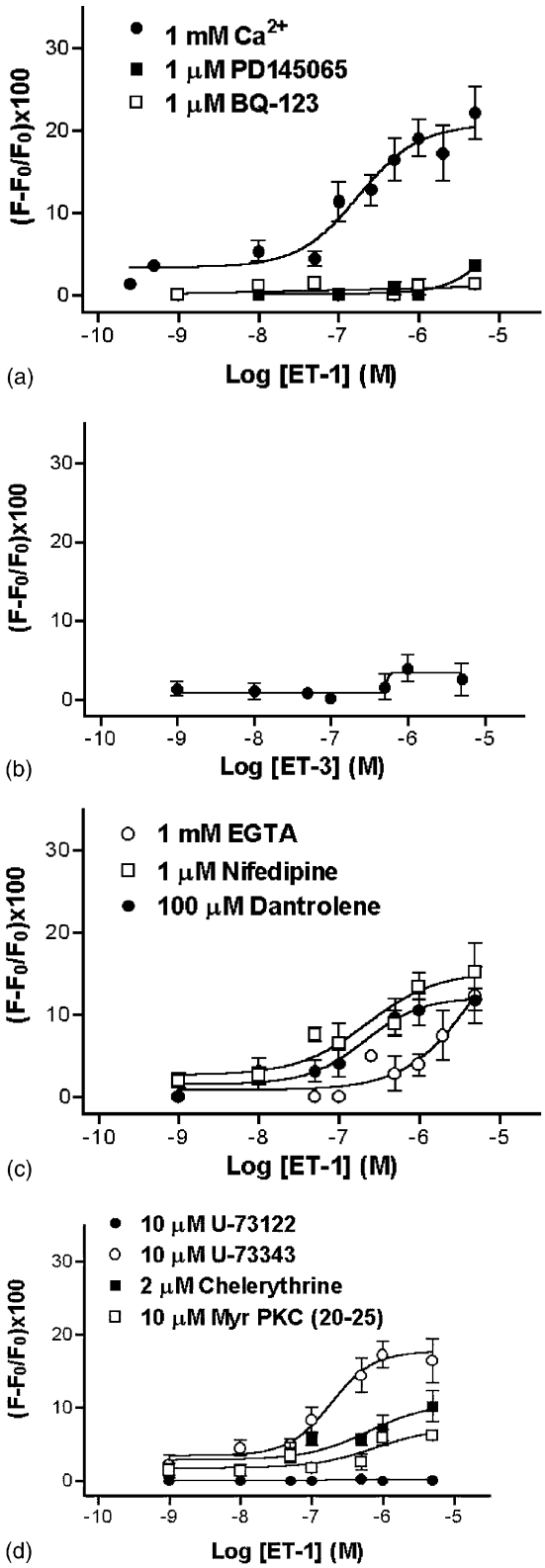

Fig. 4. Concentration–response curves of ET-1 and ET-3 actions on $[Ca^{2+}]_i$ and effects of various experimental conditions. Fluo-3-loaded cells were detached and harvested by low-speed centrifugation. Resuspended cells were analysed on a FACScan flow cytometer as described under "Section 2". Fluo-3 fluorescence was measured before and 1–2 s after the addition of ETs. *F*, Fluo-3 fluorescence after ET stimulation; F_0, basal Fluo-3 fluorescence. (a) ET-1 concentration–response curves in control conditions (buffer containing 1 mM $CaCl_2$) or in the presence of an ETR antagonist (1 μM PD-145065 or BQ-123). (b) ET-3 concentration–response curve. (c) ET-1 concentration–response curves in the presence of 1 mM EGTA without $CaCl_2$, 1 μM nifedipine or 100 μM dantrolene. (d) ET-1 concentration–response curves in the presence of 10 μM U-73122, 10 μM U-73343 (negative control of U-73122), 2 μM chelerythryne or 10 μM myr-PKC(20–28). The non-linear regression analysis of the GraphPad Prism computer program was used to fit concentration–response curves and derive EC_{50} values. The data points represent the means ± SEM of at least three independent experiments.

convert Fluo-3 fluorescence values into absolute $[Ca^{2+}]_i$. The average basal $[Ca^{2+}]_i$ was 110.80 ± 8.51 nM (N = 15). ET-1 elicited a concentration-dependent increase of fluorescence (Fig. 4, panel a), which reached the maximal effect at 1 μM. The EC_{50} value was 176.00 ± 2.03 nM (N = 6) with a Hill coefficient of 1.1. As illustrated in Fig. 4 (panel a), the ET-1-induced increase of fluorescence was abolished by both a non-selective (PD-145065) and an ET_A-selective (BQ-123) antagonist. BQ-123 (1 μM) completely blocked the effect of 5 μM ET-1. ET-3 was not able to increase the fluorescent signal within a concentration range of 1–1000 nM, while at higher concentrations a modest increase of fluorescence was detectable (Fig. 4, panel b). These results suggest that in cardiomyoblasts the ET-1-stimulated variation of $[Ca^{2+}]_i$ is mainly mediated through activation of ET_A receptors.

The mode of ET-1-induced $[Ca^{2+}]_i$ increase in cardiomyoblasts linked to ET_A receptors was examined evaluating the role of extra- and intracellular Ca^{2+} sources. Removal of extracellular Ca^{2+} (in the presence of 1 mM EGTA) induced a profound modification of ET-1 concentration–response curve (Fig. 4, panel c), which was shifted to the right and did not reach the maximal effect seen in control experiments. The estimated EC_{50} value of 5.34 μM (N = 3) was 30-fold higher than that obtained in control experiments. Thus, ET-1 potency was negatively influenced by a Ca^{2+}-free medium, suggesting a partial dependence of the response upon extracellular Ca^{2+} inflow. Cell pretreatment with 1 μM nifedipine to inhibit L-type VOCCs caused a shift to the right in the ET-1 concentration–response curve and a decrease of the maximal fluorescence (Fig. 4, panel c). The calculated EC_{50} value was 228.00 ± 2.11 nM (N = 3). The potency of the agonist and its maximal effect were reduced by cell treatment with nifedipine. Similarly, cell preincubation with 100 μM dantrolene, a blocker of RyRs, caused a decrease of ET-1 potency as well as a reduction in its maximal effect. The concentration–response curve in response to ET-1 (Fig. 4, panel c) was shifted to the right, and the derived EC_{50} value was 210.30 ± 2.10 nM (N = 3).

U-73122 has been shown to inhibit receptor-mediated PLC activation in various cell types [32–34]. As shown in Fig. 4 (panel d), ET-1-induced increase of fluorescence was completely abolished by cardiomyoblast preincubation with U-73122 (10 μM). To verify the specificity of U-73122 effect, we treated cardiomyoblasts with U-73343, a close

structural analogue of U-73122, which does not inhibit PLC [32,35]. U-73343 (10 μM) had a modest effect on ET-1-induced increase of fluorescence, slightly reducing its maximal efficacy (EC_{50} value 183.10 ± 7.70 nM, N = 3) (Fig. 4, panel d). This result suggests that ET_A-mediated variation of $[Ca^{2+}]_i$ is triggered by activation of PLC resulting in generation of IP_3, thereby realising Ca^{2+} through IP_3-gated channels located on endoplasmic reticulum (ER).

Stimulation of PLC in response to occupation of ETRs is associated with intracellular generation of both IP_3 and DG, followed by PKC activation. In turn, PKC-mediated pathways may modulate L-type VOCCs [36]. Indeed, in rat ventricular myocytes both ET-1 and a DG analogue increase L-type Ca^{2+} current through activation of PKC [37]. Therefore, it was important to substantiate a possible role of PKC in ET-1-induced increase of $[Ca^{2+}]_i$ in H9c2 cardiomyoblasts. However, cell pretreatment with an inhibitor of PKC, calphostin C (50 nM), induced a shift of cell distribution within the viable cell gate (data not shown). The amount of viable, apoptotic and necrotic cells were unmodified by treatment with calphostin C but ET-1 caused a variable and inconsistent increase of fluorescence. Using the binding of PE-labelled annexin V to cell membrane phosphatidylserine [28], we verified that the shifted cells were in a very early phase of apoptosis (data not shown). Thus, chelerithryne (2 μM) and myr-PKC(20–28)

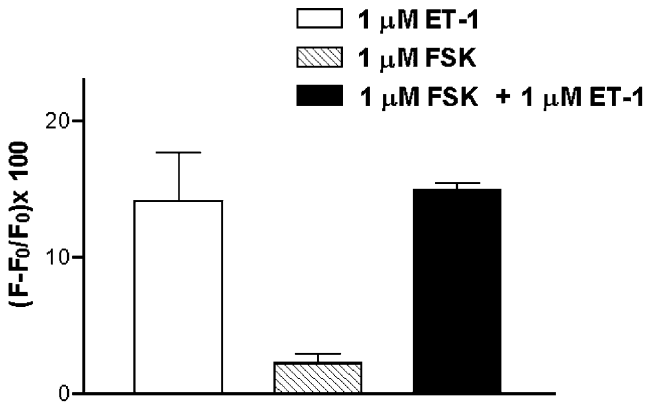

Fig. 5. Effect of forskolin on basal and ET-1-stimulated $[Ca^{2+}]_i$. Cell suspensions were preincubated for 5 min at room temperature in the presence and absence of 1 μM forskolin before stimulation with and without 1 μM ET-1. Cell fluorescence was analysed on a FACScan flow cytometer as described under "Section 2". *F*, Fluo-3 fluorescence after addition of forskolin, ET-1 or forskolin plus ET-1; F_0, basal Fluo-3 fluorescence. Data points represent the means ± SEM of three independent experiments.

(10 μM) were used to inhibit PKC [38–40]. Chelerithryne is a selective PKC inhibitor while myr-PKC(20–28) is specific for PKC-α and PKC-β. Both agents affected the concentration–response curves of ET-1, reducing both potency and maximal effect (Fig. 4, panel d). The derived

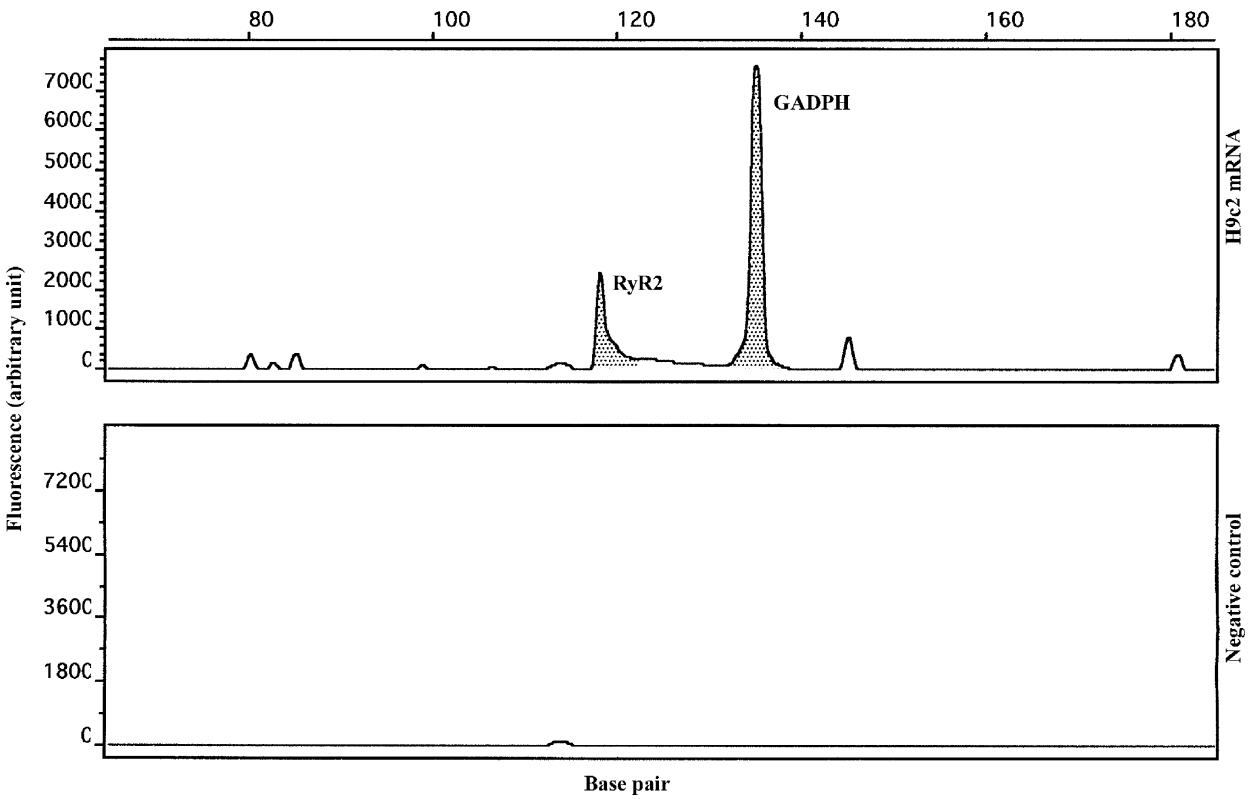

Fig. 6. RT–PCR detection of the RyR_2 transcript in H9c2 cardiomyoblasts. RNA was isolated cardiomyoblasts as described under "Section 2". PCR products generated by primers designed to amplify sequences of specific genetic messages for RyR_2 and GADPH (control) were fractionated on capillary electrophoresis and detected by fluorescence measurement. The area of each peak is proportional to the amount of each transcript. The negative control represents the result obtained with no RNA but with reverse primers.

EC_{50} values for chelerithryne and myr-PKC(20–28) inhibition of ET-1 effect were 778.50 ± 2.60 nM (N = 3) and 615.10 ± 2.56 nM (N = 3), respectively.

Forskolin, a stimulator of adenylyl cyclases, has been shown to induce an increment of the inward Ca^{2+} currents in H9c2 cadiomyoblsts [14], implying the involvement of cAMP in L-type VOCC modulation. We tested whether 1 μM forskolin was able to cause an increase of fluorescence of Fluo-3-loaded cells. Pretreatment of cells did not induce any significant increase of basal fluorescence and did not modify the stimulatory response of 1 μM ET-1 (Fig. 5). Furthermore, forskolin did not affect the dose–response curve of ET-1 (1 nM–5 μM; data not shown).

3.4. RyR expression in H9c2 cardiomyoblasts

Szalai *et al.* [16] have reported that RyR mRNA is not detectable until after cardiomyoblasts differentiate into myotubes. However, we observed an effect of dantrolene on ET-1-induced increase of $[Ca^{2+}]_i$ in H9c2 cells from subconfluent cultures, which suggests the presence of RyRs in these cells. Further supporting this idea, [^{3}H]ryanodine bound to cardiomyoblast membranes (15 fmol/mg proteins, N = 2). Using RT–PCR, we identified RyR_2 mRNA from subconfluent cell cultures (Fig. 6). Similar results were obtained from two independent batches of cultures. Although the amount of mRNA encoding for RyR_2 present in cardiomyoblasts was significantly lower than that in rat myocardium (data not shown), the presence of this mRNA correlates to the functional effect of the RyR blocker, dantrolene.

4. Discussion

In the present study, we show that H9c2 cardiomyoblasts express ETRs mainly of the ET_A subtype which are functionally coupled to rise of $[Ca^{2+}]_i$. To measure $[Ca^{2+}]_i$ variations in cardiomyoblast suspensions, a cytofluorimetric method based on the use of the Ca^{2+} indicator Fluo-3 was adopted [27]. Repeated measurements and tests to verify cell viability demonstrated the validity of this method for studying $[Ca^{2+}]_i$ in H9c2 cells. In this assay, we examined the plateau of the Ca^{2+} response.

Stimulation of cells with ET-1 induced a concentration-dependent rise of $[Ca^{2+}]_i$ which was inhibited by both non-selective and ET_A-selective antagonists indicating that ET-1 acts through the ET_A receptor. The observation that ET-3 did not cause a similar concentration-dependent increase of $[Ca^{2+}]_i$ further supports the exclusive activation ET_A receptors by ET-1.

The pharmacological characterisation of the binding site revealed that both ET-3 and BQ-788, an ET_B-selective antagonist, inhibited [^{125}I]ET-1 binding with low potency, while the ET_B-selective agonist, IRL-1620, was ineffective as inhibitor. On the other hand, under similar experimental conditions we have shown that IRL-1620 completely displaced [^{125}I]ET-1 binding to rat cerebellar membranes [41]. Low amounts of ET_B receptors were detectable by western blotting in membranes prepared from H9c2 cardiomyoblasts. However, this ETR subtype did not show the classical pharmacological characteristics of the rat cerebellar ET_B receptor and was not functionally coupled to increase of $[Ca^{2+}]_i$. It is possible that cardiomyoblasts express an atypical or immature form of the ET_B receptor subtype.

ET-1 caused a concentration-dependent rise of $[Ca^{2+}]_i$ *via* a mechanism involving PLC activation and release of Ca^{2+} from IP_3-gated intracellular stores. The addition of U-73122, a PLC inhibitor, completely blocked the ET-1-induced response indicating that the increase of $[Ca^{2+}]_i$ is secondary to activation of PLC. The initiating event appears to be the increased production of IP_3 that binds to IP_3 receptor (IP_3R) Ca^{2+} channels on the ER with consequent opening of these channels and release of Ca^{2+}. Following this trigger, other processes influence and maintain the agonist-induced increase of $[Ca^{2+}]_i$. The involvement of extracellular Ca^{2+} entry was supported by the marked shift to the right of ET-1 concentration–response curve in the absence of extracellular Ca^{2+} (Fig. 4). Various types of plasma membrane Ca^{2+} channels may be responsible for Ca^{2+} inflow, including L-type VOCCs. Nifedipine caused a shift to the right of ET-1 concentration–response curve decreasing both its potency and efficacy (Fig. 5). Whereas the potency reduction was modest the effect of nifedipine on ET-1 efficacy was more consistent. A marked activity of this dihydropyridine Ca^{2+} channel inhibitor could not be expected, since cardiomyoblasts from subconfluent cultures are known to have a modest expression of L-type VOCCs [16]. These channels are also modulated by PKC-mediated pathway [36,42]. In rat ventricular myocytes, both ET-1 and a DG analogue increase L-type Ca^{2+} current through activation of PKC [37]. Using cell-permeable PKC inhibitors we verified whether ET-1-induced activation of PKC to cause opening L-type VOCCs or other membrane Ca^{2+} channels. One PKC inhibitor, calphostin C, induced cell apoptosis at a concentration corresponding to the IC_{50} for PKC inhibition, while chelerithryne and myr-PKC(20–28) modified ET-1 concentration–response curves, causing a reduction of both potency and maximal efficacy. In the presence of these PKC inhibitors, ET-1 potency decreased by 3- to 4-fold. These data indicate that in cardiomyoblasts PKC exerts a positive regulation on membrane Ca^{2+} channels.

Since the L-type Ca^{2+} current of H9c2 cardiomyoblsts is augmented by the β-adrenergic agonist, isoproterenol, *via* cAMP [14], we examined the effect of forskolin on variation of $[Ca^{2+}]_i$. Forskolin did not cause any increase of $[Ca^{2+}]_i$ and did not modify the Ca^{2+} response induced by ET-1. Thus, our results do not support any involvement of cAMP-dependent phosphorylation of L-type Ca^{2+} VOCCs as suggested by Hescheler *et al.* [14]. We can also exclude a

role of cAMP-activated plasma membrane Ca^{2+} channels in rising $[Ca^{2+}]_i$ in cardiomyoblasts. Since protein kinase A (PKA) phosphorylates IP_3Rs with consequent enhancement of IP_3-induced Ca^{2+} release in various cell types [43], we could expect to detect an additive effect of forskolin on ET-1-induced $[Ca^{2+}]_i$ rise. However, this was not the case in our experimental conditions, either for inability to measure the initial transient peak of $[Ca^{2+}]_i$ rise or for reaching the maximal activation of IP_3R Ca^{2+} channels.

Although H9c2 cardiomyoblasts in subconfluent cultures do not completely express Ca^{2+} channels with the cardiac phenotype [15,16], we tested whether cell treatment with dantrolene, a RyR inhibitor, affected the response to ET-1. Surprisingly, dantrolene caused a shift to the right of the ET-1 concentration–response curve, notably reducing the ET-1 efficacy. Thus, RyRs appeared to release Ca^{2+} in response to ET-1 stimulation. Local rise of $[Ca^{2+}]_c$ as consequence of IP_3R Ca^{2+} channels opening may induce RyRs on ER to open and release more Ca^{2+}. As in the case of plasma membrane L-type VOCCs, RyRs do not play a major role in maintaining the increase of $[Ca^{2+}]_i$ induced by ET-1. A functional coupling between L-type VOCCs and RyRs may exist in these modestly differentiated cells, which may result in the similar effects of nifedipine and dantrolene. However, we had a serious problem with these functional results since Szalai *et al*. [16] reported that RyR mRNA is not detectable in undifferentiated cardiomyoblasts. Therefore, we examined [^{3}H]ryanodine binding to cardiomyoblast membranes and the presence of RyR_2 mRNA obtained from subconfluent cultures. Both binding assays and RT–PCR suggested the presence of low amounts of RyRs in H9c2 cardiomyoblasts. Differences of cell culture conditions and/or RT–PCR assays may explain the discrepancy between our results and previous reported observations [16].

Our findings demonstrate that H9c2 cardiomyoblasts express a high proportion of ET_A receptors. In this embryonic cell line, ET_A receptors are functionally coupled to rise of $[Ca^{2+}]_i$ through activation of PLC and PKC. Since ET-1 exerts clear positive inotropic effects on myocardium acting through ET_A receptors [22], and the cardiac ET-1/ET_A receptor system is involved in heart hypertrophy and failure [21,22], H9c2 cell line may represent an useful *in vitro* model to study the role of ET-1 system in cardiac pathophysiology. This cell model may also be used to improve our knowledge on regulation of Ca^{2+} homeostasis and its importance in hypertrophic response in cardiac cells.

Acknowledgments

We thank Dr. H.E. Hamm and Dr. P. Migliorini for helpful discussions. This work was supported by Italian Ministry of University, Scientific and Technological Research (M.U.R.S.T.) Grant No. 9805249947 (to M.R.M.).

References

[1] Yanagisawa M, Kurihara H, Kimura S, Tombe T, Kobajashi M, Mitsui Y, Yazaki Y, Goto J, Masaki T. A novel potent vasoconstrictor peptide produced by vascular endothelial cells. Nature 1988;332:411–5.
[2] Inoue A, Yanagiswa M, Kimura S, Kasuya Y, Miyauchi T, Goto K, Masaki T. The human endothelin family: three structurally and pharmacologically distinct isopeptides predicted by separate genes. Proc Natl Acad Sci USA 1989;86:2863–7.
[3] Pollock DM, Keith TL, Highsmith RF. Endothelin receptor and calcium signaling. FASEB J 1995;9:1196–204.
[4] Gray GA, Battistini B, Webb DJ. Endothelins are potent vasoconstrictors and much more besides. Trends Pharmacol Sci 2000;21:38–40.
[5] Sokolovsky M. Endothelin receptor subtypes and their role in transmembrane signaling mechanisms. Pharmacol Ther 1995;68:435–71.
[6] Rubanyi GM, Polokoff MA. Endothelins: molecular biology, biochemistry, pharmacology, physiology and pathophysiology. Pharmacol Rev 1994;46:325–415.
[7] Webb ML, Meek TD. Inhibitors of endothelin. Med Res Rev 1997;17:17–67.
[8] Minowa T, Miwa S, Kobayashi S, Enoki T, Zhang XF, Komuro T, Iwamuro Y, Masaki T. Inhibitory effect of nitrovasodilators and cyclic GMP on ET-1-activated Ca^{2+}-permeable nonselective cation channel in rat aortic smooth muscle cells. Br J Pharmacol 1997;120:1536–44.
[9] Russell FD, Molenaar P. The human heart endothelin system: ET-1 synthesis, storage, release and effects. Trends Pharmacol Sci 2000;21:353–9.
[10] Molenaar P, O'Reilly G, Sharkey A, Kuc RE, Harding DP, Plumpton C, Gresham GA, Davenport AP. Characterization and localization of endothelin receptor subtypes in the human atrioventricular conducting system and myocardium. Circ Res 1993;72:526–38.
[11] Serneri GG, Cecioni I, Vanni S, Paniccia R, Bandinelli B, Vetere A, Janming X, Bertolozzi I, Boddi M, Lisi GF, Sani G, Modesti PA. Selective upregulation of cardiac endothelin system in patients with ischemic but not idiopathic dilated cardiomyopathy: endothelin-1 system in the human failing heart. Circ Res 2000;86:377–85.
[12] Hilal-Dandan R, Merck DT, Lujan JP, Brunton LL. Coupling of the type A endothelin receptor to multiple responses in adult rat cardiac myocytes. Mol Pharmacol 1994;45:1183–90.
[13] Hilal-Dandan R, Ramirez MT, Villegas S, Gonzalez A, Endo-Mochizuki Y, Brown JH, Brunton LL. Endothelin ET_A receptor regulates signaling and ANF gene expression via multiple G protein-linked pathways. Am J Physiol 1997;272:H130–7.
[14] Hescheler J, Meyer R, Plant S, Krautwurst D, Rosenthal W, Schultz G. Morphological, biochemical, and electrophysiological characterization of a clonal cell (H9c2) line from rat heart. Circ Res 1991;169:1476–86.
[15] Menard C, Pupier S, Mornet D, Kitzmann M, Nargeot J, Lory P. Modulation of L-type calcium channel expression during retinoic acid-induced differentiation of H9C2 cardiac cells. J Biol Chem 1999;274:29063–70.
[16] Szalai G, Csordas G, Hantash BM, Thomas AP, Hajnoczky G. Calcium signal transmission between ryanodine receptors and mitochondria. J Biol Chem 2000;275:15305–13.
[17] Tran K, Zha X, Chan M, Choy PC. Enhancement of phospholipid hydrolysis in vasopressin-stimulated BHK-21 and H9c2 cells. Mol Cell Biochem 1995;151:69–76.
[18] Reilly BA, Brostrom MA, Brostrom CO. Regulation of protein synthesis in ventricular myocytes by vasopressin. The role of sarcoplasmic/endoplasmic reticulum Ca^{2+} stores. J Biol Chem 1998;273:3747–55.
[19] Chen WC, Chen CC. Signal transduction of arginine vasopressin-induced arachidonic acid release in H9c2 cardiac myoblasts: role of Ca^{2+} and the protein kinase C-dependent activation of p42 mitogen-activated protein kinase. Endocrinology 1999;140:1639–48.

[20] Brostrom MA, Reilly BA, Wilson FJ, Brostrom CO. Vasopressin-induced hypertrophy in H9c2 heart derived myocites. Int J Biochem Cell Biol 2000;32:993–1006.
[21] Rothermund L, Pinto YM, Hocher B, Vetter R, Leggewie S, Kobetamehl P, Orzechowski HD, Kreutz R, Paul M. Cardiac endothelin system impairs left ventricular function in renin-dependent hypertension via decreased sarcoplasmic reticulum Ca^{2+} uptake. Circulation 2000;102:1582–8.
[22] Giannessi D, Del Ry S, Vitale RL. The role of endothelins and their receptors in heart failure. Pharmacol Res 2001;43:111–26.
[23] Lowry OH, Rosebrough NJ, Farr A, Randall RJ. Protein measurement with folin phenol reagent. J Biol Chem 1951;193:265–75.
[24] Mazzoni MR, Breschi MC, Ceccarelli F, Lazzeri N, Giusti L, Nieri P, Lucacchini A. Suc-[Glu^{9},$Ala^{11,15}$]-endothelin-1 (8-21), IRL 1620, identifies two populations of ET_B receptors in guinea-pig bronchus. Br J Pharmacol 1999;127:1406–14.
[25] Zucchi R, Yu G, Ghelardoni S, Ronca F, Ronca-Testoni S. Effect of MEN 10755, a new disaccharide analogue of doxorubicin, on sarcoplasmic reticulum Ca^{2+} handling and contractile function in rat heart. Br J Pharmacol 2000;131:342–8.
[26] Laemmli UK. Cleavage of structural proteins during the assembly of the head of bacteriophage T4. Nature 1970;227:680–5.
[27] Vandenberghe PA, Ceuppens JL. Flow cytometric measurement of cytoplasmic free calcium in human peripheral blood T lymphocytes with fluo-3, a new fluorescent calcium indicator. J Immunol Methods 1990;127:197–205.
[28] Koopman G, Reutelingsperger CP, Kuijten GA, Keehnen RM, Pals ST, Van Oers MH. Annexin V for flow cytometric detection of phosphatidylserine expression on B cells undergoing apoptosis. Blood 1994;84:1415–20.
[29] McPherson GA. Analysis of radioligand binding experiments. A collection of computer programs for the IBM PC. J Pharmacol Methods 1985;14:213–28.
[30] Cheng YC, Prusoff WH. Relationship between the inhibition constant (K_i) and the concentration of inhibitor which causes 50% inhibition (IC_{50}) of an enzymatic reaction. Biochem Pharmacol 1973;22:3099–108.
[31] Kochl R, Alken M, Rutz C, Krause G, Oksche A, Rosenthal W, Schulein R. The signal peptide of the G protein-coupled human endothelin B receptor is necessary for translocation of the N-terminal tail across the endoplasmic reticulum membrane. J Biol Chem 2002;277:16131–8.
[32] Bleasdale JE, Thakur NR, Gremban RS, Bundy GL, Fitzpatrick FA, Smith RJ, Bunting S. Selective inhibition of receptor-coupled phospholipase C-dependent processes in human platelets and polymorphonuclear neutrophils. J Pharmacol Exp Ther 1990;255:756–68.
[33] Yule DI, Williams JA. U73122 inhibits Ca^{2+} oscillations in response to cholecystokinin and carbachol but not to JMV-180 in rat pancreatic acinar cells. J Biol Chem 1992;267:13830–5.
[34] Macrez N, Morel JL, Mironneau J. Specific $G\alpha_{11}\beta_3\gamma_5$ protein involvement in endothelin receptor induced phosphatidylinositol hydrolysis and Ca^{2+} release in rat portal vein myocytes. Mol Pharmacol 1999;55:684–92.
[35] Smith RJ, Sam LM, Justen JM, Bundy GL, Bala GA, Bleasdale JE. Receptor-coupled signal transduction in human polymorphonuclear neutrophils: effects of a novel inhibitor of phospholipase C-dependent processes on cell responsiveness. J Pharmacol Exp Ther 1990;253:688–97.
[36] Barritt GJ. Receptor-activated Ca^{2+} inflow in animal cells: a variety of pathways tailored to meet different intracellular Ca^{2+} signaling requirements. Biochem J 1999;337:153–69.
[37] He JQ, Pi Y, Walker JW, Kamp TJ. Endothelin-1 and photoreleased diacylglycerol increase L-type Ca^{2+} current by activation of protein kinase C in rat ventricular myocytes. J Physiol 2000;524:807–20.
[38] Herbert JM, Augereau JM, Gleye J, Maffrand JP. Chelerythrine is a potent and specific inhibitor of protein kinase C. Biochem Biophys Res Commun 1990;172:993–9.
[39] Ward NE, O'Brian CA. Inhibition of protein kinase C by *N*-myristoylated peptide substrate analogs. Biochemistry 1993;32:11903–9.
[40] Gupta KP, Ward NE, Gravitt KR, Bergman PJ, O'Brian CA. Partial reversal of multidrug resistance in human breast cancer cells by an *N*-myristoylated protein kinase C-α pseudosubstrate peptide. J Biol Chem 1996;271:2102–11.
[41] Ceccarelli F, Giusti L, Bigini G, Costa B, Grillotti D, Fiumalbi E, Lucacchini A, Mazzoni MR. Regulation of agonist binding to rat ET_B receptors by cations and GTPγS. Biochem Pharmacol 2001;62:537–45.
[42] Keef KD, Hume JR, Zhong J. Regulation of cardiac and smooth muscle Ca^{2+} channels (Ca_V1.2a,b) by protein kinases. Am J Physiol Cell Physiol 2001;281:C1743–56.
[43] Wojcikiewicz RJ, Luo SG. Phosphorylation of inositol 1,4,5-trisphosphate receptors by cAMP-dependent protein kinase. Type I, II, and III receptors are differentially susceptible to phosphorylation and are phosphorylated in intact cells. J Biol Chem 1998;273:5670–7.